

Available online at www.sciencedirect.com**SciVerse ScienceDirect**

Procedia Environmental Sciences 18 (2013) 809 – 817

Procedia

Environmental Sciences

2013 International Symposium on Environmental Science and Technology (2013 ISEST)

Formation of zero-valent iron nanoparticles mediated by amino acids

Karolina Machalova Siskova^{a,*}, Jana Straska^a, Michal Krizek^b, Jiri Tucek^b,
Libor Machala^b, Radek Zboril^a

^aRegional Centre of Advanced Technologies and Materials, Dept. of Physical Chemistry, Faculty of Science, University of Palacky, Olomouc 78371, Czech Republic

^bRegional Centre of Advanced Technologies and Materials, Dept. of Experimental Physics, RCPTM, Faculty of Science, University of Palacky, Olomouc 78371, Czech Republic

Abstract

Zero-valent iron nanoparticles (NZVI) which are frequently investigated for their application potential in pollutants removal can be prepared by several different ways. Here, we report NZVI formation by wet chemical synthesis in the presence of selected L-amino acids, thus low-molecular weight and biocompatible species. According to our results based mainly, but not only, on Mössbauer spectroscopy (an excellent iron sensitive method), there are distinct differences in zero-valent iron content when each of the amino acids under study mediated NZVI formation. The content of iron atoms in the oxidation state of zero is one of crucial parameters when considering the reductive mode of NZVI action against pollutants. For instance, while the presence of L-glutamic acid promoted NZVI generation, L-cysteine hindered it completely. The effect of L-arginine and L-glutamine presence during NZVI formation was also investigated and evaluated. Moreover, the influence of acidic and alkaline pH values on NZVI formation in the presence of all four selected L-amino acids was looked into. It turned out that acidic and alkaline pH values have negative effects on NZVI formation in the presence of L-glutamic acid and L-glutamine. On the contrary, almost no effect of pH was observed for L-cysteine and L-arginine.

© 2013 The Authors. Published by Elsevier B.V. Open access under [CC BY-NC-ND license](https://creativecommons.org/licenses/by-nc-nd/4.0/).
Selection and peer-review under responsibility of Beijing Institute of Technology.

Keywords: zerovalent iron; nanoparticle synthesis; Moessbauer spectroscopy; ZVI; L-amino acids.

1. Introduction

The environment is highly polluted by many different species which come from human activities and current lifestyle. It is of an utmost importance to persuade people to respect the environment and to clean

* Corresponding author. Tel.: +420-585-634-955; fax: +420-585-634-958.
E-mail address: karolina.siskova@upol.cz

it up in order to achieve a sustainable world. One of the possibilities how to effectively remove increased contents of contaminants from water and/or soil, such as halogenated organic compounds, heavy metal cations, arsenic, antibiotics, personal care products etc., is the use of nanoscale zero-valent iron particles (NZVI) [1-4]. Indeed, the reduction ability of iron in the oxidation states of 0 and +2 is exploited together with the sorption capacity of iron corrosion products resulting from the transformation of NZVI in water (mainly iron oxides and oxyhydroxides) and co-precipitation of pollutants with them [1-7].

Since NZVI particles would be unstable under ambient conditions (i.e. full air and humidity access), it is usually stabilized by a protective shell for the sake of better handling and storage. Regardless the NZVI preparation procedure performed either in oven, or in solution, the protective shell can consist of inorganic oxide layer [8], polymers and polyelectrolytes [9-19]. The deposition of another metal over zero-valent iron core can be also employed and lead to increased NZVI reactivity with pollutants as known from the literature [20-22].

Recently, we have demonstrated that L-glutamic acid mediating NZVI generation by wet chemical synthesis is also able to augment the reactivity of NZVI in water, increase the reaction rate of trichloroethylene removal while maintaining the stability of NZVI for a period of 9 months [23]. By this approach we have created double-shell NZVI particles consisting of zero-valent iron core, inner inorganic shell (iron oxide/hydroxide), and outer organic shell [23]. The use of L-amino acids as mediators of NZVI formation was not accidental, but inspired by the facts that L-amino acids are environmentally friendly species and are able to bind chemically to the surface of iron oxide nanoparticles [24-28].

In the present work, we investigate and evaluate the influence of the presence of four L-amino acids, applied separately, and pH values of the starting iron-bearing solution on the NZVI formation. The L-amino acids serving as mediators of NZVI generation are as follows: L-glutamic acid, L-glutamine, L-arginine, L-cysteine. Encouraged by our recent great results achieved with L-glutamic acid [23], we have chosen L-glutamine mediating NZVI formation for the sake of a direct comparison of the influence of one of the two carboxylic groups absence. Furthermore, L-arginine and L-cysteine are used in order to see the effect of guanidyl group and thiol group presence during NZVI generation, respectively. Each of these L-amino acids bears a different charge when dissolved at pH 2, neutral pH and pH 10. Therefore, also this factor is looked into and the resulting iron-containing particles are thoroughly characterized and mutually compared. Since there have been no published papers about that topic yet, we believe that the novelty and significance is obvious. Our results and discussion are based on several different experimental techniques, such as Mössbauer spectroscopy (an excellent iron sensitive technique), scanning electron microscopy (SEM), and nitrogen adsorption/desorption isotherms analyzed by BET (Brunauer-Emmett-Teller) method.

2. Experimental

L-glutamic acid, L-glutamine, L-arginine, L-cysteine, and sodium borohydride were purchased from Sigma-Aldrich. Sodium hydroxide, hydrochloric acid, and ferrous sulphate heptahydrate were obtained from Penta. All chemicals were used as received without any further purification. All glassware was cleaned by diluted hydrochloric acid (1/1 v/v).

The preparation procedure of NZVI mediated by a particular L-amino acid was performed in a very similar way and under the same experimental conditions as described previously in [23]. Briefly, the appropriate amount of a particular L-amino acid was dissolved in 10 mL of deionized water (pH 6) in order to obtain 20 mM concentration of L-amino acid. Then 0.27785 g of $\text{FeSO}_4 \cdot 7\text{H}_2\text{O}$ was added in the freshly prepared 10 mL L-amino acid solution. Ferrous sulphate was allowed to dissolve for 10 min while stirring at 500 rpm. In the meantime, 0.46 g of NaBH_4 was dissolved in 40 mL of deionized water placed in an ice-bath. The mixture of ferrous sulphate and the particular L-amino acid was then quickly added into the cold aqueous NaBH_4 solution while vigorous stirring (900 rpm). All syntheses proceeded under

ambient conditions and were repeated at least five times to get statistically relevant samples which were further characterized. The resulting precipitates were either magnetically separated, or centrifuged (in the case of nonmagnetic samples) at 10,000 rpm for 10 min at 23 °C, washed with acetone, and dried in vacuum overnight. The resulting powders were further stored in closed vials under ambient conditions. The effect of pH values was investigated by the following approach: the aqueous solutions of pH 2 and/or pH 10 were prepared. Subsequently, these solutions were used for the preparation of all reactant solutions. The samples are labeled as: GluNZVIpH2, GluNZVIpH6, GluNZVIpH10, GlnNZVIpH2, GlnNZVIpH6, GlnNZVIpH10, ArgNZVIpH2, ArgNZVIpH6, ArgNZVIpH10, CysNZVIpH2, CysNZVIpH6 and CysNZVIpH10 according to the particular L-amino acid and pH value.

The transmission ^{57}Fe Mössbauer spectra were measured using a home-made Mössbauer spectrometer in a constant acceleration mode with a $^{57}\text{Co}(\text{Rh})$ source. The isomer shift values were related to metallic alpha iron at room temperature. The measurements were carried out at room temperature (300 K) and without the application of any external magnetic field. The samples for Mössbauer spectroscopy were prepared with a great care concerning the constant amount and thickness.

Surface areas were determined by nitrogen adsorption at 77.4 K using static volumetric technique on a Sorptomatic 1990 analyzer (Thermo Finnigan). Prior to the measurements, the samples were degassed with turbomolecular pump at room temperature for at least 20 h. The adsorption-desorption isotherms were measured up to the saturation pressure of nitrogen. The values of specific surface area were determined by the multipoint BET (Brunauer-Emmett-Teller) method within the range of 0.05-0.50 of relative pressures. Analyses were performed with the ADP (Advanced Data Processing) 4.0 software package (CE Instruments).

Morphologies of the as-prepared samples were investigated employing a Hitachi SU 660 scanning electron microscope working at 5 kV.

3. Results and discussion

The powdered samples were characterized by Mössbauer spectroscopy. The spectra for all samples are shown in Fig. 1, the appropriate parameters are summarized in Table 1. In general, from the fit of experimentally obtained Mössbauer spectra, it can be determined the atomic ratio (with the error of ± 1 at.%) of iron in any oxidation and spin states. Taking into account the reductive mode of iron particles action against pollutants, the determination of Fe^0 and Fe^{II} vs. Fe^{III} oxidation states is very important and cannot be correctly determined by any other experimental technique. In our case, Mössbauer spectroscopy revealed two well-resolved spectral components in almost all the samples except from CysNZVI where only one spectral component could be used to best fit the experimental data (Figure 1, Table 1). While the sextets in Figure 1 and Table 1 can be unambiguously attributed to alpha-Fe [29], the hyperfine parameters of the doublet subspectra are characteristic for paramagnetic and/or superparamagnetic high-spin ferric oxide/oxyhydroxide [30]. It is obvious from Figure 1 and Table 1 that the samples differ mostly in relative contents of the two identified phases, i.e. Fe^0 and Fe^{III} . While all GluNZVI samples manifested themselves by the highest zero-valent iron content under all three pH values applied, all CysNZVI samples consisted only of ferric component.

Furthermore, it is clearly seen from Table 1 that acidic and alkaline pH values of the mixtures consisting of the particular L-amino acid and ferrous sulphate which is consequently reduced by sodium borohydride have significantly negative effects on NZVI generation in the case of GluNZVI and GlnNZVI when the atomic ratio of Fe^0 vs. Fe^{III} of the resulting iron particles considered and compared with those generated from the mixture of neutral pH value. On the contrary, the effect of the mixture pH value is almost negligible in the case of CysNZVI and ArgNZVI. We hypothesize that the accessibility of carboxylic group/s and simultaneous presence and/or absence of positive charge on amino group might

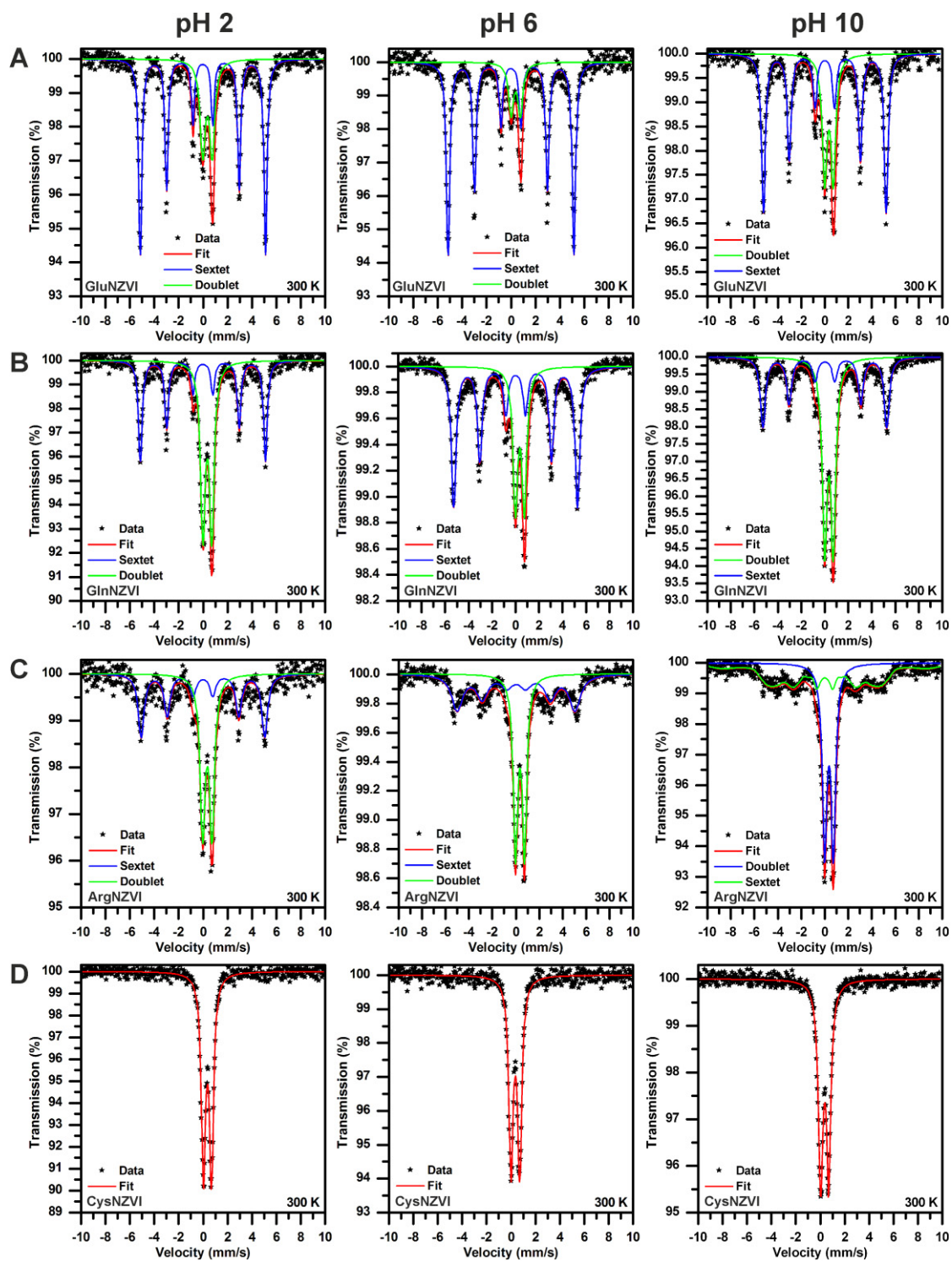


Fig. 1. Mössbauer spectra of (A) GluNZVI, (B) GlnNZVI, (C) ArgNZVI, (D) CysNZVI prepared in the presence of selected L-amino acids dissolved in the ambient indicated above the images, i.e. pH 2, pH 6 (neutral), pH 10.

play a role in the formation of an intermediate complex between the particular L-amino acid and ferrous sulphate. This intermediate complex if formed can be reduced by sodium borohydride in the next step of the preparation procedure. It turned out that thiol group of L-cysteine has very little effect on NZVI generation if in its protonated and/or deprotonated form.

Table 1. Mössbauer parameters, assignment of iron-containing phases, atomic percentage of each iron-containing phase, specific surface areas obtained from BET analysis.

Sample name	Spectral component	Isomer shift [mm/s]	Quadrupole splitting [mm/s]	Hyperfine magnetic field [T]	Line width [mm/s]	Assignment	Atomic ratio ± 1 [%]	Specific surface area [m ² /g]
GluNZVIpH2	Sextet	0.00	0.00	31.9	0.31	α -Fe ⁰	72	30 \pm 3
	Doublet	0.36	0.77	-	0.52	Fe ^{III}	28	
GluNZVIpH6	Sextet	0.00	0.00	32.1	0.34	α -Fe ⁰	84	30 \pm 3
	Doublet	0.39	0.76	-	0.49	Fe ^{III}	16	
GluNZVIpH10	Sextet	0.00	0.00	32.5	0.40	α -Fe ⁰	67	59 \pm 4
	Doublet	0.36	0.74	-	0.49	Fe ^{II}	33	
GlnNZVIpH2	Sextet	0.00	0.00	31.9	0.37	α -Fe ⁰	48	84 \pm 3
	Doublet	0.35	0.72	-	0.46	Fe ^{III}	52	
GlnNZVIpH6	Sextet	0.00	0.00	32.8	0.49	α -Fe ⁰	67	32 \pm 3
	Doublet	0.37	0.76	-	0.49	Fe ^{III}	33	
GlnNZVIpH10	Sextet	0.00	-0.01	32.8	0.52	α -Fe ⁰	44	93 \pm 4
	Doublet	0.36	0.73	-	0.50	Fe ^{III}	56	
ArgNZVIpH2	Sextet	0.00	0.00	31.5	0.59	α -Fe ⁰	48	104 \pm 5
	Doublet	0.35	0.77	-	0.50	Fe ^{III}	52	
ArgNZVIpH6	Sextet	0.03	-0.02	31.2	1.15	α -Fe ⁰	50	110 \pm 5
	Doublet	0.36	0.76	-	0.46	Fe ^{III}	50	
ArgNZVIpH10	Sextet	0.00	0.00	32.1	0.40	α -Fe ⁰	50	126 \pm 7
	Doublet	0.36	0.74	-	0.46	Fe ^{III}	50	
CysNZVIpH2	Doublet	0.36	0.66	-	0.41	Fe ^{III}	100	118 \pm 6
CysNZVIpH6	Doublet	0.36	0.71	-	0.43	Fe ^{III}	100	133 \pm 7
CysNZVIpH10	Doublet	0.36	0.66	-	0.45	Fe ^{III}	100	120 \pm 6

Characteristic morphologies of the samples are presented in Fig.2. There are three main morphological features: spherical particles, leave-like plates, and needle-like shapes (Figure 2). While spherical particles arranged into 2D-chains can be assigned to zero-valent iron particles [23]; the other shapes are characteristic for ferric oxide/oxyhydroxides. The atomic ratio of Fe⁰:Fe^{III} (Table 1) determined on the basis of Mössbauer spectroscopy is in a fairly good correspondence with the observed morphologies, i.e. (i) the higher content of Fe⁰, the higher amount of 2D-chains consisting of spherical particles and (ii) the higher content of Fe^{III}, the increased presence of non-spherical shapes encountered. Some of the images seem to be fuzzy because of very tiny particles whose size is below the resolution of the employed microscope. These tiny particles are attached to the surface of differently shaped morphologies (Fig. 2).

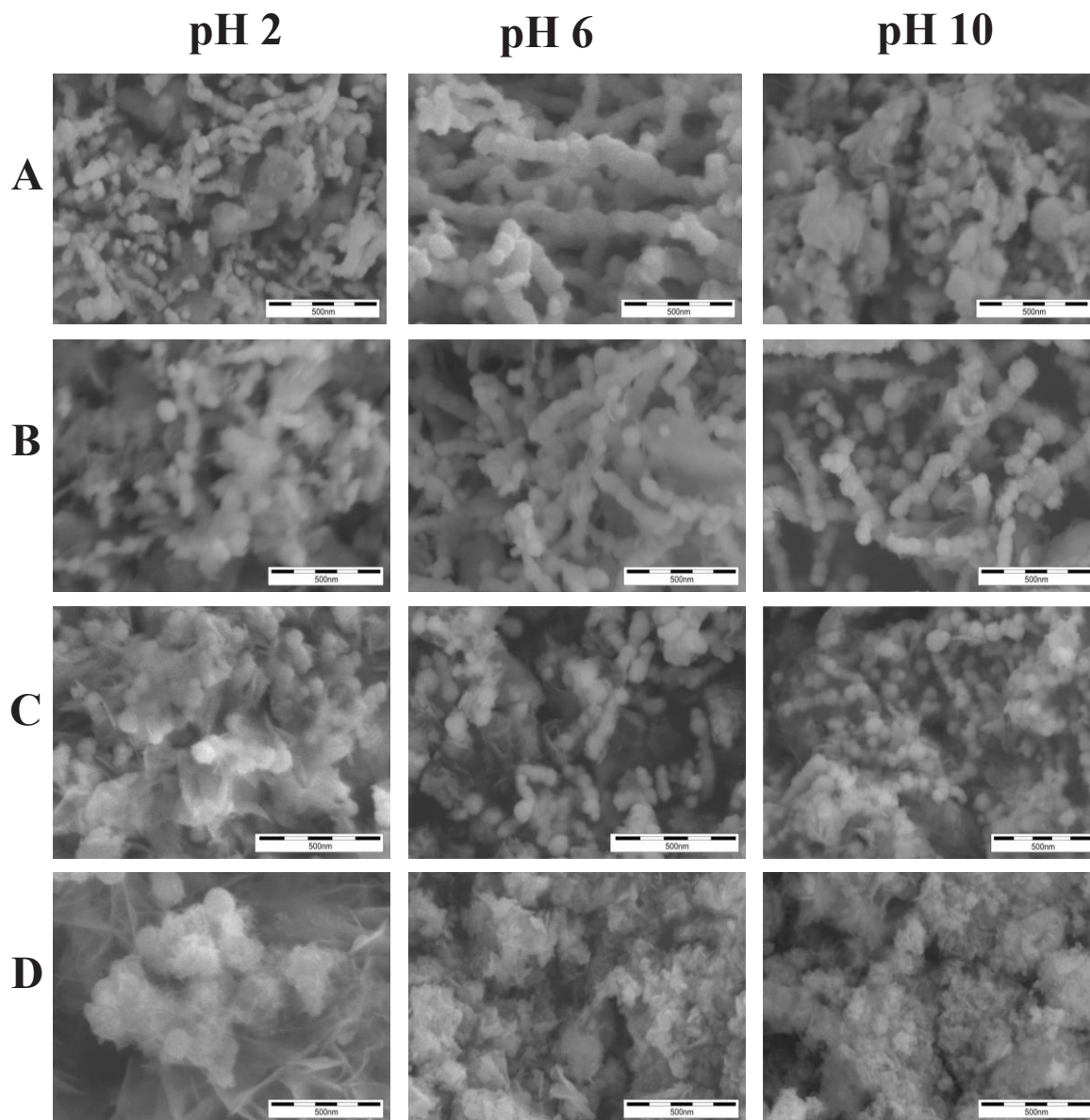


Fig. 2. Scanning electron microscopic images of (A) GluNZVI, (B) GlnNZVI, (C) ArgNZVI, (D) CysNZVI prepared in the presence of selected amino acids dissolved in the ambient indicated above the images, i.e. pH 2, pH 6 (neutral), pH 10. Scale bar is 500 nm in all images.

Due to the same scale of the presented SEM images (Fig.2), it can be clearly seen that both, acidic and alkaline pH values of the mixture of L-amino acid and ferrous sulphate, influenced the size of the resulting particles in the samples to some extent. Particularly in the case of GluNZVI, the generated

particles were bigger when prepared from the mixtures of neutral pH value than from those of acidic and alkaline pH values (Fig. 2). It should be reminded at this place that except from the pH value of the L-amino acid and ferrous sulphate mixture the other conditions were kept exactly the same in all three cases. Therefore, the observed changes in the size of spherical particles in GluNZVI samples were purely caused by pH value of the mixture. This implicitly corroborates the above-suggested hypothesis about a specific role of two carboxylic groups of L-glutamic acid during the intermediate complex formation and consequently NZVI generation. The influence of the mixture pH value was less significant in the case of GlnNZVI and ArgNZVI samples. However, there are still noticeable size differences among GlnNZVI and ArgNZVI samples (Fig. 2). In the case of CysNZVI, there was a big difference between morphologies obtained at pH 2 vs. the others as demonstrated in Fig. 2.

Specific surface area which is a very important characteristic for the evaluation of NZVI reactivity is reported in the last column of Table 1. These values were determined from nitrogen gas adsorption and desorption isotherms using BET analysis. At first glance, the samples containing a higher amount of Fe^0 than Fe^{III} revealed the lowest ($\sim 30 \pm 3 \text{ m}^2/\text{g}$) specific surface area values (Table 1). This can be explained by the fact that particles of zero-valent iron are highly aggregated due to strong magnetic interactions as already shown in [23]. The samples possessing a ratio of $\text{Fe}^0:\text{Fe}^{\text{III}}$ at around 1:1 manifested themselves by the specific surface area values in the range between 84 and $110 \pm 5 \text{ m}^2/\text{g}$. The last group of samples possessing the highest specific surface area values ($\sim 120 \pm 6 \text{ m}^2/\text{g}$ and higher) is formed mainly by CysNZVI which contained only ferric component at all three pH values under study. The two exceptions from the just-mentioned arrangement into three main groups according to specific surface area values given in correlation with the sample composition are GluNZVIpH10 and ArgNZVIpH10. Interestingly, both exceptional samples were prepared using the reaction mixture of pH 10 and revealed a higher specific surface area values than expected when considering their composition solely. According to SEM images (Figure 2), rather small particles were formed especially in GluNZVIpH10 and ArgNZVIpH10 samples. We believe that pH 10 induced a rapid precipitation of ferrous ions and their subsequent oxidation in the mixtures of the particular L-amino acid and ferrous sulphate, i.e. already before the chemical reduction took place.

It can be summarized that the pH value of the iron-bearing reactant (either in the form of an intermediate complex with a particular L-amino acid, or as aqua complex) solution is a highly important parameter which greatly influence the results of the NZVI preparation procedure performed in the presence of different kinds of L-amino acids. We presume that the samples efficiency of pollutants removal (e.g. trichloroethylene degradation) will be completely different depending on their Fe^0 vs. Fe^{III} ratio, particle shapes and sizes.

4. Conclusions

It can be concluded that the choice of L-amino acid mediating the generation of iron particles is crucial for the content of Fe^0 in the resulting samples. From the four L-amino acids under study, L-glutamic acid highly promoted the Fe^0 generation. On the contrary, L-cysteine acting as a mediator of iron particles generation induced ferric oxides/oxyhydroxides formation only. L-glutamine and L-arginine presence during iron particles generation resulted in the $\text{Fe}^0:\text{Fe}^{\text{III}}$ ratios which fall between the two edges constituted by L-glutamic acid and L-cysteine systems. These results point at the importance of the chemical structure of each L-amino acid and its role during dissolution of ferrous sulphate.

Furthermore, the pH value of the mixtures of a particular L-amino acid and ferrous sulphate was varied (pH 2 and/or pH 10 vs. pH 6) and the consequences investigated. The effect of L-glutamic acid and L-cysteine mediating NZVI generation on the resulting systems remained the same under acidic and alkaline pH values of the mixture, i.e. the highest $\text{Fe}^0:\text{Fe}^{\text{III}}$ ratios obtained for L-glutamic acid, while only ferric component present in the case of L-cysteine. The greatest impact of mixture pH value was observed

for the systems containing L-glutamic acid and L-glutamine. This can be again related to their chemical structure.

Acknowledgements

Ing. Monika Dosedelova is thanked for SEM images. Financial support by P108/11/P657 Grant awarded by GACR, the project of the Ministry of Industry and Business of the Czech Republic (project ID: FR-TI3/196), the Operational Program Research and Development for Innovations - European Regional Development Fund (project CZ.1.05/2.1.00/03.0058 of the Ministry of Education, Youth and Sports of the Czech Republic), and the projects of the Technology Agency of the Czech Republic (project ID: TE01020218) is gratefully acknowledged.

References

- [1] Zhang L, Fang M. Nanomaterials in pollution trace detection and environmental improvement. *Nano Today* 2010; **5**: 128-142.
- [2] Tratnyek PG, Johnson RL. Nanotechnologies for environmental cleanup. *Nano Today* 2006; **1**: 44-8.
- [3] Li L, Fan M, Brown RC, Van Leeuwen JH, Wang J, Wang W et al. Synthesis, properties, and environmental applications of nanoscale iron-based materials: a review. *Crit. Rev. Environ. Sci. Technol.* 2006; **36**, 405-31.
- [4] Zhang WX. Nanoscale iron particles for environmental remediation: an overview. *J. Nanopart. Res.* 2003; **5**: 323-32.
- [5] Noubactep C. Processes of contaminant removal in "Fe⁰-H₂O" systems revisited: the importance of co-precipitation. *The Open Environmental Journal* 2007; **1**: 9-13.
- [6] Noubactep C. The fundamental mechanism of aqueous contaminant removal by metallic iron. *Water SA* 2010; **36**: 663-70.
- [7] Noubactep C. Aqueous contaminant removal by metallic iron: is the paradigm shifting? *Water SA* 2011; **37**: 419-26.
- [8] Kim HS, Ahn JY, Hwang KY, Kim IK, Hwang I. Atmospherically stable nanoscale zero-valent iron particles formed under controlled air contact: characteristics and reactivity. *Environ. Sci. Technol.* 2010; **44**: 1760-6.
- [9] Comba S, Di Molfetta A, Sethi R. A comparison between field applications of nano-, micro- and millimetric zero-valent iron for the remediation of contaminated aquifers. *Water Air Soil Pollut* 2011; **215**: 595-607.
- [10] Geng G, Jin Z, Li T, Qi X. Preparation of chitosan-stabilized Fe⁰ nanoparticles for removal of hexavalent chromium in water. *Sci. Total Environ.* 2009; **407**: 4994-5000.
- [11] Ghauch A, Tuqan A, Assi HA. Antibiotic removal from water: elimination of amoxicillin and ampicillin by microscale and nanoscale iron particles. *Environ. Pollut.* 2009; **157**: 1626-35.
- [12] He F, Zhao D. Manipulating the size and dispersibility of zerovalent iron nanoparticles by use of carboxymethylcellulose stabilizers. *Environ. Sci. Technol.* 2007; **41**: 6216-21.
- [13] Kim HJ, Phenrat T, Tilton RD, Lowry GV. Fe⁰ nanoparticles remain mobile in porous media after aging due to slow desorption of polymeric surface modifiers. *Environ. Sci. Technol.* 2009; **43**: 3824-30.
- [14] Phenrat T, Long TC, Lowry GV, Veronesi B. Partial oxidation ("aging") and surface modification decrease the toxicity of nanosized zerovalent iron. *Environ. Sci. Technol.* 2009; **43**: 195-200.
- [15] Saleh N, Phenrat T, Sirk K, Dufour B, Ok J, Sarbu T et al. Adsorbed triblock copolymers deliver reactive iron nanoparticles to the oil/water interface. *Nano Lett.* 2005; **5**: 2489-94.
- [16] Schrick B, Hydutsky BW, Blough JL, Mallouk TE. Delivery vehicles for zerovalent metal nanoparticles in soil and groundwater. *Chem. Mater.* 2004; **16**: 2187-93.
- [17] Sun YP, Li XQ, Zhang WX, Wang HP. A method for the preparation of stable dispersion of zero-valent iron nanoparticles. *Colloids Surf. A* 2007; **308**: 60-6.
- [18] Tiraferri A, Chen KL, Sethi R, Elimelech M. Reduced aggregation and sedimentation of zero-valent iron nanoparticles in the presence of guar gum. *J. Colloid Interface Sci.* 2008; **324**: 71-9.
- [19] Wang W, Thou M, Jin Z, Li T. Reactivity characteristics of poly(methyl methacrylate) coated nanoscale iron particles for trichloroethylene remediation. *J. Hazard. Mater.* 2010; **173**: 724-30.

- [20] Katsenowich YP, Miralles-Wilhel FR. Evaluation of nanoscale zerovalent iron particles for trichloroethylene degradation in clayey soils. *Sci. Total Environ.* 2009; **407**; 4986-93.
- [21] Lien HL, Zhang W. Nanoscale iron particles for complete reduction of chlorinated ethenes. *Colloid Surf. A* 2001; **191**; 97-105.
- [22] Schrick B, Blough JL, Jones AD, Mallouk TE. Hzdrechlorination of trichloroethylene to hydrocarbons using bimetallic nickel-iron nanoparticles. *Chem. Mater.* 2002; **14**; 5140-7.
- [23] Siskova K, Tucek J, Machala L, Otyepkova E, Filip J, Safarova K et al. *J. Nanopart. Res.* 2012; **14**; 805.
- [24] Durmus Z, Kavas H, Toprak MS, Baykal A, Alticekic TG, Aslan A et al. L-lysine coated iron oxide nanoparticles: synthesis, structural and conductivity characterization. *J. Alloys Compd.* 2009; **484**; 371-6.
- [25] Manton A, Gozzo F, Schmitt B, Stern WB, Gerber Y, Robin AY et al. Amino acids in iron oxide mineralization: (incomplete) crystal phase selection is achieved even with single amino acids. *J. Phys. Chem. C* 2008; **112**; 12104-10.
- [26] Marinescu G, Patron L, Culita DC, Neagoe C, Lepadatu CI, Balint I et al. Synthesis of magnetite nanoparticles in the presence of aminoacids. *J. Nanopart. Res.* 2006; **8**; 1045-51.
- [27] Sousa MH, Tourinho FA, Rubim JC. Use of Raman micro-spectroscopy in the characterization of $M^II Fe_2O_4$ ($M = Fe, Zn$) electric double layer ferrofluids. *J. Raman Spectrosc.* 2000; **31**; 185-191.
- [28] Wang Z, Zhu H, Wang X, Yang F, Yang X. One-pot green synthesis of biocompatible arginine-stabilized magnetic nanoparticles. *Nanotechnology* 2009; **20**; 465606.
- [29] Schneeweiss O, Zboril R, Mashlan M, Petrovsky E, Tucek J. Novel solid-state synthesis of α -Fe and Fe_3O_4 nanoparticles embedded in a MgO matrix. *Nanotechnology* 2006; **17**; 607-16.
- [30] Cornell RM, Schwertmann U. *The iron oxides: structure, properties; reactions, occurrence and uses.* 2nd ed. Weinheim: Wiley-VCH Publishers; 2003.